

SIGNATURE PAGE

This thesis for honors recognition has been approved for the

Department of Mathematics, Engineering, & Computer science



Director

5/1/17

Date

Anthony M. Spilka

Reader

5/1/17

Date



Reader

5/1/17

Date

Creating the Tools to Study Galaxy Evolution
Through Examination of Properties of Dark Matter

Halos

Joseph Zepeda

May 1, 2017

Abstract

We study dark matter galaxy halos found by Jared W. Coughlin while running the Amiga Halo Finder on the output of a modified GADGET 2 large scale simulation [5], [7], [6]. The neighborhood of the halos is defined at different redshifts by using a structure finding algorithm developed by Dr. Lara A. Phillips' group [4]. We use Python to examine how halos vary when in a cluster or a filament and to develop analytical tools that allow us to determine whether specified halos are in-falling into a major cosmic web node. We find that in the recent past the most massive halos are in clusters while in the most distant past the most massive halos are in filaments. This indicates continued heavy in-fall of material in and from filaments as massive halos form at cosmic web nodes.

Contents

1 List of Figures	4
2 List of Variables	6
3 Introduction	7
4 Data	8
5 Methods and Results	12
6 Future work	23
7 Conclusion	23

1 List of Figures

1	Example of particle assignment to possible halo center [1]. The elliptical lines represent equal density (isodensity) contours and the x's represent particles. Note that the black circle with radius $\frac{D}{2}$ is not an isodensity line, but rather represents the region where particles are checked to see if they are bound to the leftmost prospective halo. The figure shows that the leftmost prospective halo checks to see if the particles as far from it as halfway between it and the center prospective halo are gravitationally bound.	10
2	Halos Bullocks spin vs. Classical spin with classification shown by color. The unclassified halos are shown in black, the cluster halos are shown in green, and the filament halos are shown in blue.	13
3	Halo positions with velocity direction denoted by arrows. Black halos are in clusters and red halos are in filaments.	14
4	Halo position with mass denoted by size of dot and classification by color. Black halos are in clusters and red halos are in filaments.	15
5	Halo positions with velocity direction denoted by arrows. Black halos are in clusters and red halos are in filaments.	16
6	Halo positions with velocity direction denoted by arrows. Black halos are in clusters and red halos are in filaments.	17
7	Halo positions with velocity direction denoted by arrows. Black halos are in clusters and red halos are in filaments.	18
8	Halo position and mass at varying redshifts. Black halos are in clusters and red halos are in filaments.	19

9	Halo position and mass at varying redshifts. Black halos are in clusters and red halos are in filaments.	20
10	Halo position and mass at varying redshifts. Black halos are in clusters and red halos are in filaments.	21
11	Halo position and mass at varying redshifts. Black halos are in clusters and red halos are in filaments.	22

2 List of Variables

z : Redshift, $z = \frac{R_0}{R(t)} - 1$

R_0 : Current scale of the universe = 1

$R(t)$: Scale of the universe in comparison to the present scale, a function of time

$\varphi(r)$ Gravitational potential energy, a function of radius

K_E : Kinetic energy $K_E = \frac{1}{2}mv^2$

G : Newton's Gravitational Constant

R_{vir} : Radius at which the density reaches normal space density

M_{vir} : Virial mass, mass contained in the virial radius

3 Introduction

After the Big Bang the universe was filled with a nearly uniform distribution of hydrogen, helium, and dark matter. Due to the force of gravity these particles began to collapse together to form regions of denser material. After enough time passed these particles became dense enough for galaxies to form. These denser regions are called halos. A halo includes hydrogen and helium, but is mostly comprised of dark matter by mass. Dark matter is responsible for between 80% and 95% of the mass of a halo. Because dark matter comprises such a high percentage of the mass of a halo and gravity plays such a big role in shaping the universe, dark matter is the most important factor in how halos move and change through time.

Most of the hydrogen, helium, and dark matter particles did not exist in regions of high enough density to form a halo. Instead, these particles formed string-like regions with densities above that of the initial uniform distribution, yet still much lower than that of the halos. As more time passed these strings grew large through gravity and eventually started connecting and forming nodes. The nodes tend to be denser than the individual strings due to the attractive force of gravity between the strings. We name these strings *filaments*, and these nodes *clusters*. The filaments and clusters make up what we call the cosmic web. As filaments connect with each other and form nodes, the particles both in the filaments and around nodes are pulled toward the nodes. We call these particles and even halos that are pulled into clusters *in-falling material*. We call the areas that experience this pull *infall regions*.

Since the Big Bang space has been expanding, not just in the sense of growing larger but in a stretching sense. For example, if you think of space as the surface of a balloon and consider two points on the this surface, then as the balloon expands the space between these points is stretched. Because of this “stretching” of space, light that was emitted in the past will appear to be stretched when we see it. This stretching of light gives it a longer wavelength and we call this *redshift* because red has

longest wavelength of visible light. So, more red-shifted light means it was emitted further away, and thus we are seeing light that was emitted further in the past. As we observe light from the earlier universe we see high redshifts. We calculate redshift by the following formula:

$$z = \frac{R_0}{R(t)} - 1. \quad (1)$$

Here z is the redshift, R_0 is the current scale of the universe normalized as 1, and $R(t)$ is the size of the universe at some time t as compared to R_0 . For example, a value of $z = 3$ would correspond to the universe being a quarter of its current size. Therefore larger z values indicate light that was emitted further in the past.

We seek to study dark matter galaxy halo properties as a function of redshift in and outside of in-fall regions along filaments and in clusters. By studying halos we hope to get a better understanding of what happens to galaxies as halos move through different regions of space. We first look at halo properties at each redshift as a function of neighborhood (filament, cluster, or undetermined) defined by the structure of the surrounding gas. We then identify in-fall regions around cosmic web nodes and study those regions and the large halo that forms within them.

4 Data

The halos we studied were found by Jared Coughlin using AMIGA’s Halo Finder on data generated by GADGETS 2 large-scale simulations, an N-body simulator that uses a hierarchical tree algorithm to determine the gravitational forces [5], [7], [6] [1]. Each halo’s neighborhood was categorized as either a filament region, a cluster region, or an undefined region at different redshifts by using a structure finding algorithm developed by Dr. Phillips’ group [4].

The AMIGA’s Halo Finder (AHF) applies Newton’s law of gravity and the expansion of the universe to an initial set of dark matter, gas, and star “particles” that

represent a region of the universe. Note that dark matter obeys the laws of gravity just like the other particles so we don't treat it any different than them in our simulation. Since these are the main forces that these "particles" experience we can use this to simulate how this region changes at different redshifts.

There is of course no analytical solution for the gravitational field of a system with this many particles so AHF numerically approximates the solution. To make the approximation less computationally intensive AHF uses an adaptive mesh. This helps minimize the time spent approximating what happens in the areas with low density. AHF does six refinements of its mesh for each time step. The adaptive mesh grid is defined by areas of the same density. By defining the grid in this way finding possible halo centers just requires checking local density maxima.

AHF assumes spherical symmetry for the density of the mass around the possible halo centers. Particles are assigned to a possible halo if they are within a circle centered at the possible halo's center with radius equal to half the distance to the nearest other possible halo center. Figure 1 shows an example of this.

Next, AHF determines which particles are bound by solving for the particle's gravitational potential φ . Gravitational potential is the energy an object with a mass of 1 kg would have if its position was changed from its current position to the place with no gravitational potential. For example, a ball with mass m that is some distance above the floor has gravitational potential and thus a gravitational potential energy of φm . If we were to let the ball fall to the floor its gravitational potential would be converted into kinetic energy. Note that kinetic energy $K_E = \frac{1}{2}mv^2$, where K_E is kinetic energy, m is the mass of the object, and v is its velocity. If an object has a kinetic energy greater than its gravitational potential energy it must be unbound. So therefore for an object of mass m and velocity v if $K_E = \frac{1}{2}mv^2 > \varphi m$ then the object is unbound. Therefore, if the object had a velocity such that $v > \sqrt{2\varphi}$ then the object is unbound. We call the minimum velocity needed to be unbound, escape

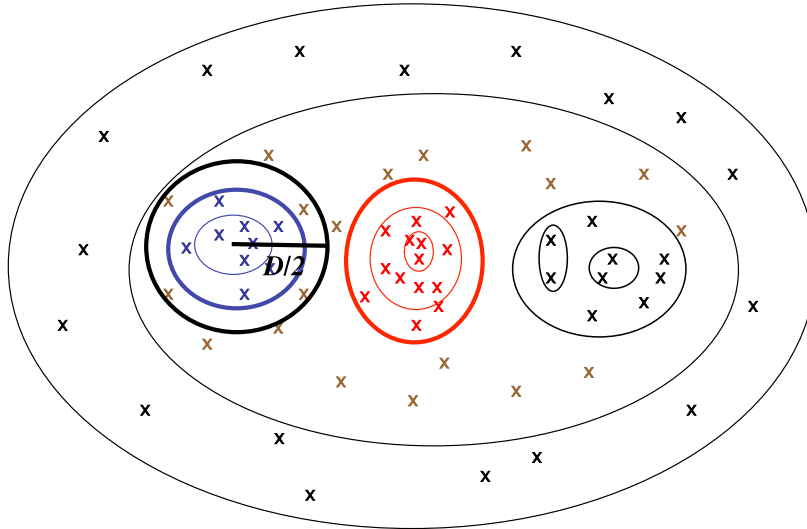


Figure 1: Example of particle assignment to possible halo center [1]. The elliptical lines represent equal density (isodensity) contours and the x's represent particles. Note that the black circle with radius $\frac{D}{2}$ is not an isodensity line, but rather represents the region where particles are checked to see if they are bound to the leftmost prospective halo. The figure shows that the leftmost prospective halo checks to see if the particles as far from it as halfway between it and the center prospective halo are gravitationally bound.

velocity and denote that v_{esc} .

To solve for the gravitational potential we solve Poisson's equation for $\nabla^2\varphi = 4\pi G\rho(r)$, where G is Newton's gravitational constant and ρ is the spherically symmetric density. Since φ only depends on the distance from the center of mass we can solve for φ by integrating Poisson's equation twice with respect to r . We start out with our equation:

$$\frac{1}{r^2} \frac{d}{dr} \left(r^2 \frac{d\varphi}{dr} \right) = 4\pi G\rho. \quad (2)$$

We multiply both sides by r^2 and integrate from the origin to R (the location at

which we are solving for the potential):

$$r^2 \frac{d\varphi}{dr} = 4\pi G \int_0^R \rho r^2 dr. \quad (3)$$

We rearrange and get:

$$r^2 \frac{d\varphi}{dr} = G4\pi \int_0^R \rho r^2 dr. \quad (4)$$

We note that $4\pi \int_0^R \rho r^2 dr$ is simply the total mass $M(< r)$ contained within sphere of radius r :

$$r^2 \frac{d\varphi}{dr} = GM(< r). \quad (5)$$

We divide by r^2 and integrate to get:

$$\varphi(R) = \int_0^R \frac{GM(< r)}{r^2} dr + \varphi(0). \quad (6)$$

In order to solve for φ we have to decide how we want to normalize φ . We choose to set $\varphi(\infty) = 0$ as is customary for potentials. Therefore we know the following to be true:

$$\varphi(\infty) = G \int_0^\infty \frac{M(< r)}{r^2} dr + \varphi(0) = 0. \quad (7)$$

We note that $G \int_0^\infty \frac{M(< r)}{r^2} dr = G \int_0^{R_{vir}} \frac{M(< r)}{r^2} dr + G \int_{R_{vir}}^\infty \frac{M_{vir}}{r^2} dr$, where R_{vir} and M_{vir} are virial radius and virial mass. Virial radius is the distance from the center of the halo to where the density of material approaches the density of “empty” space. Virial mass is just the mass contained inside a sphere centered at the halo with a radius equal to the virial radius. Using the aforementioned equation we can rewrite equation 5 as the following:

$$\varphi(R) = G \int_0^R \frac{M(< r)}{r^2} dr - G \int_0^{R_{vir}} \frac{M(< r)}{r^2} dr - G \int_{R_{vir}}^\infty \frac{M_{vir}}{r^2} dr. \quad (8)$$

We then subtract $G \int_0^{R_{vir}} \frac{M(<r)}{r^2} dr$ from $G \int_0^R \frac{M(<r)}{r^2} dr$ to get:

$$\varphi(R) = -G \int_R^{R_{vir}} \frac{M(<r)}{r^2} dr - G \int_{R_{vir}}^{\infty} \frac{M_{vir}}{r^2} dr. \quad (9)$$

If we evaluate the second integral we get:

$$\varphi(R) = -G \int_R^{R_{vir}} \frac{M(<r)}{r^2} dr - \frac{GM_{vir}}{R_{vir}}. \quad (10)$$

Since the prospective halo has an estimation for R_{vir} as shown in Figure 1 we can then calculate $M(<r)$ and M_{vir} from the density of the particles in R_{vir} . With these estimation we can then solve for φ and remove unbound particles. Then we can use the new outermost particle to give us a new R_{vir} and then through the same process get $M(<r)$ and M_{vir} . We can then find φ and then repeat this process until we get an sufficiently accurate approximation of the halo.

5 Methods and Results

To analyze the halo data we used Python to graph the different halo parameters. Our data has 83 parameters that describe each halo so we plotted many of these parameters against each other.

One of our plots is of the classical spin parameter, $JE^{\frac{1}{2}}G^{-1}M^{-\frac{5}{2}}$, [3] versus Bullock's spin parameter, $J/[\sqrt{2}M_{vir}R_{vir}V_{vir}]$, [2], where J , E , G , and M are total angular momentum, energy, Newton's gravitational constant, and total mass of the system. And M_{vir} , R_{vir} , and V_{vir} are virial mass, virial radius, and circular velocity at the virial radius. The classical spin parameter “is a measure of the rotation of the total halo,” and Bullock’s spin parameter is an approximation of the classical spin parameter [9]. Our plot is shown below in Figure 2.

We noticed that all classifications of halos tended to have a linear relationship

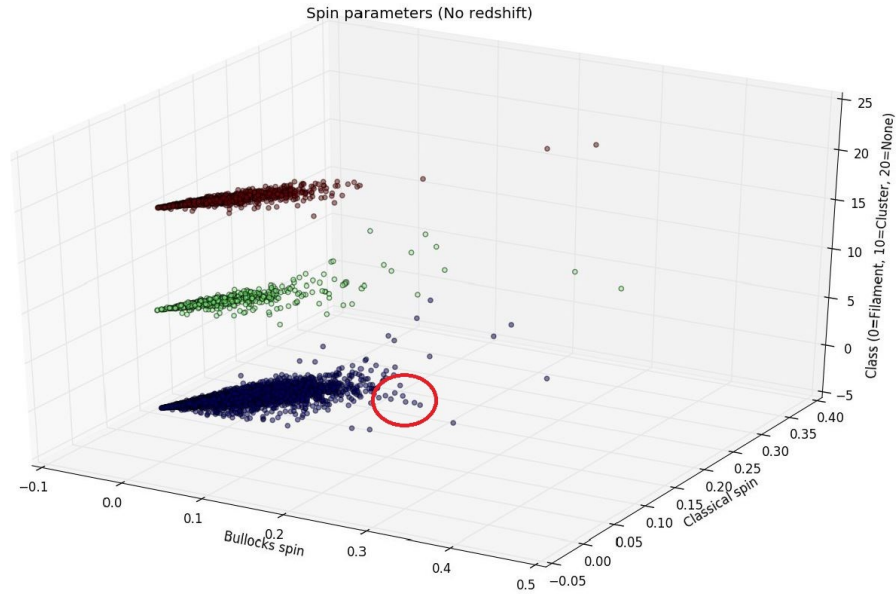


Figure 2: Halos Bullocks spin vs. Classical spin with classification shown by color. The unclassified halos are shown in black, the cluster halos are shown in green, and the filament halos are shown in blue.

between the spin parameters. However, there were a few filament halos that did not fit the linear relation between spins and appear to have no relationship between the two spins. For example, between Bullock’s spin .1 and .2 there is a group of halos with approximately the same classical spin, 0.22. This is circled in red in the Figure.

We also decided to plot halo classification, (cluster and filament), mass, position, and velocity together at different redshifts to examine how the halos changed with different surroundings. By plotting these together we hoped to see how the halos moved and changed mass and type so as to understand what halos tend to do in certain regions. Figure 3 was from the data at the highest redshift $z = 10$ meaning it was from the early universe and not long after the big bang.

The center left, center, and upper right of Figure 3 show signs of halos that are in-falling into a cluster. The halos in these regions all have velocity vectors pointing toward the same region of space. While there may not be a cluster halo or any halo in this region at that redshift we can assume that it must have quite a bit of mass

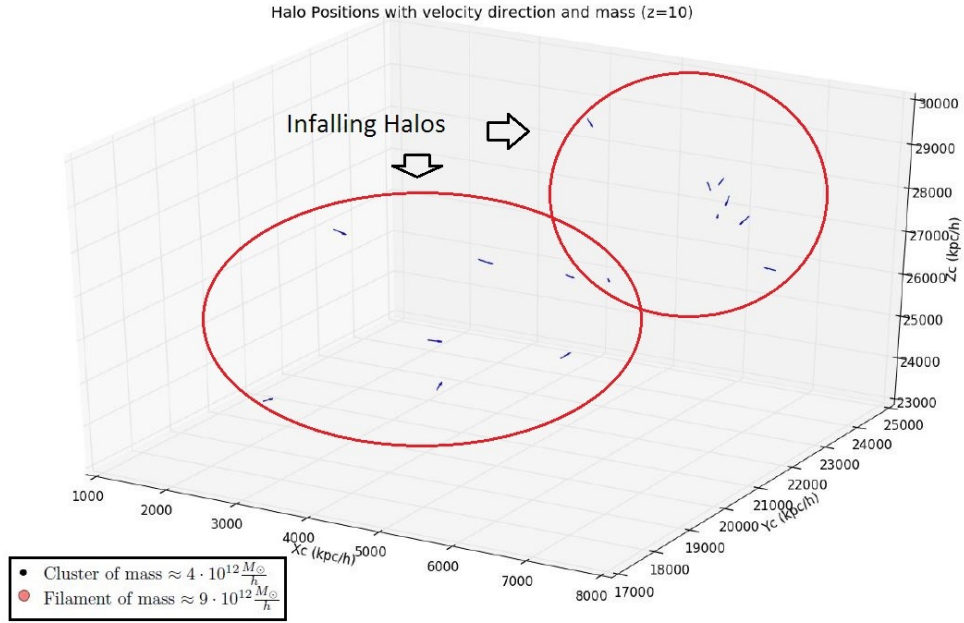


Figure 3: Halo positions with velocity direction denoted by arrows. Black halos are in clusters and red halos are in filaments.

to be pulling in all of the surrounding halos. The most massive halo in this redshift has a mass of $6.57 \cdot 10^{10} M_{\odot}/h$, where M_{\odot} is solar masses and h is a dimensionless constant that corresponds to Hubble's Constant. We use h and not the actual Hubble's constant because of the uncertainty in Hubble's constant and so the units remain right. Note that in today's terms this is an extremely small halo. The halo hasn't had enough time to grow to present halo masses. This most massive halo is in the filament in the center left of Figure 3.

As redshift decreases and we move closer to present day the masses of the halos increase. At redshift $z = 9.155$ the most massive halo remains the same place as previously mentioned with a new mass of $1.16 \cdot 10^{11} M_{\odot}/h$. The simulation does not track halos through redshifts, so we cannot say definitively which halos are which from the previous redshift. However, we assume the most massive halo is the same

halo as in the previous redshift. We make this assumption because of the position of this halo relative to the position of the halo in the previous redshift and because of the lack of other halos in that area. We continue to make this assumption for the same reasons here throughout the rest of the redshifts. We decided to name this halo Rex so that we can refer to it more easily as we track it through the redshifts.

As the redshift continues to decrease the masses continue to increase and by redshift $z = 3.946$ Rex has moved from a filament to a cluster and its mass is now $6.01 \cdot 10^{12} M_{\odot}/h$. A graph of the halos at this redshift is shown below in Figure 4.

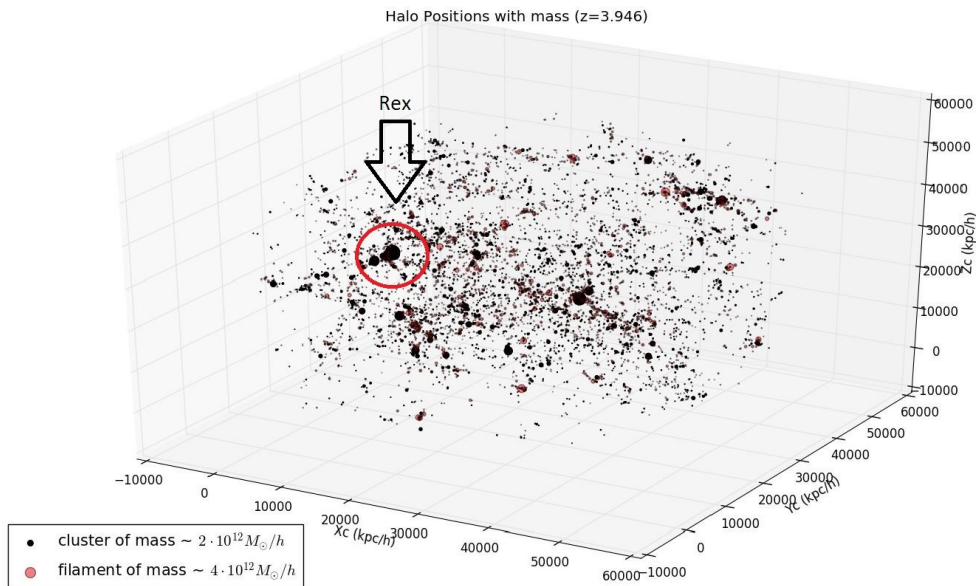


Figure 4: Halo position with mass denoted by size of dot and classification by color. Black halos are in clusters and red halos are in filaments.

Figure 4 shows that the halos have increased dramatically both in mass and number. Massive halos have formed in several regions in bunches. One other key feature of Figure 4 is the largest halos are all in clusters, which is what we expected to find. We expect this to happen because clusters form at the nodes of filaments so these regions are fed much more mass.

To get a better understanding of what was occurring at and around this massive halo we plotted the area around the halo. This can be seen in Figure 5 below.

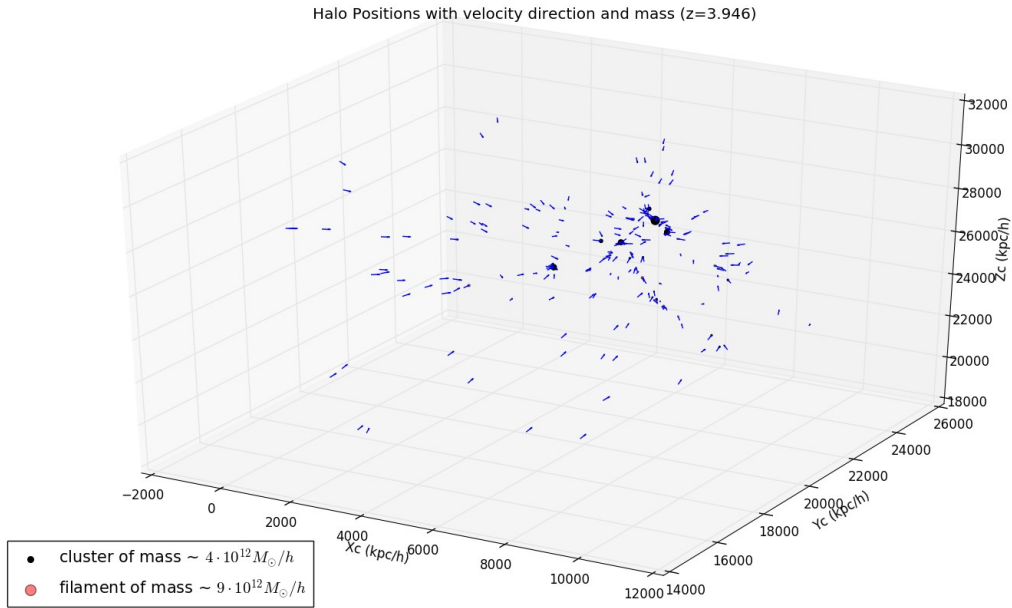


Figure 5: Halo positions with velocity direction denoted by arrows. Black halos are in clusters and red halos are in filaments.

From Figure 5 we see that Rex is near the center of a cosmic web node, with many filaments coming out of it. The halos from the filaments appear to be streaming into this cluster halo and feeding its growth in mass. To check this we looked at the number of subhalos found in this halo and found that this halo had grown from being a single halo to hosting 15 subhalos. A subhalo is what it sounds like, a halo contained in a larger halo. Since the large scale picture was too messy with large numbers of halos we continued to examine this subsection at lower redshifts.

At redshift $z = 1.409$ Rex's mass has increased nearly tenfold since the previous redshift and is now $5.61 \cdot 10^{13} M_{\odot}/h$. A number of smaller, yet still quite massive, halos have appeared in some of the surrounding space. This can be seen in the Figure 6 below.

These smaller halos are also in clusters and have masses of roughly $4 \cdot 10^{12} M_{\odot}/h$.

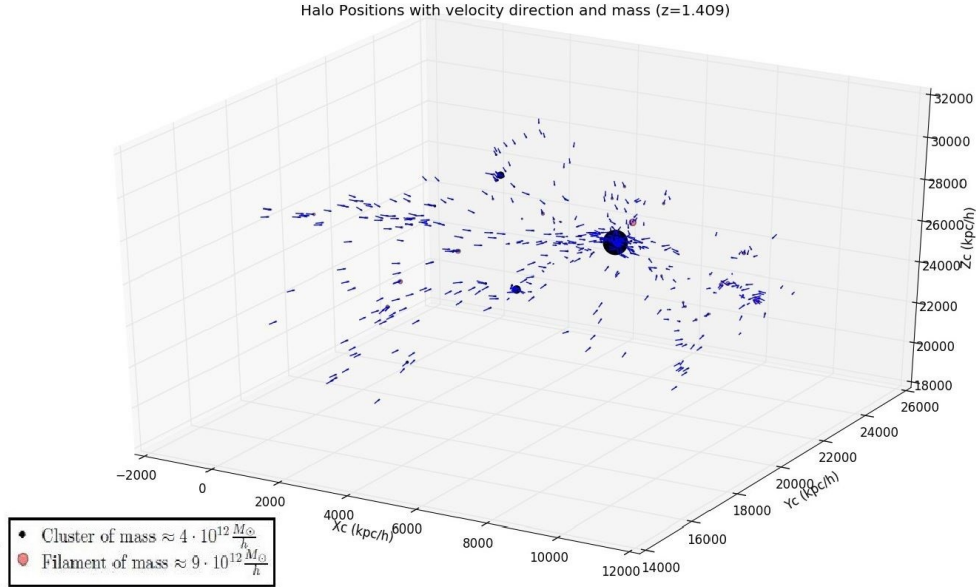


Figure 6: Halo positions with velocity direction denoted by arrows. Black halos are in clusters and red halos are in filaments.

While they are in clusters they appear to be part of filaments that are headed to the cosmic web node.

Rex has continued to be fed by in-falling halos with 80 subhalos at this redshift, $z = 1.409$. We next looked at how Rex changed throughout the rest of the redshifts in mass, location, and classification. As we examined Figure 7 we were surprised to find that at redshift $z = 0.083$ Rex is no longer classified as being in a cluster, but rather a filament; the same is true for the surrounding halos of note. We were puzzled by this at first, but after examining the plots we believe we found the reason for this.

This change in classification of the halos is probably due to a large amount of in-falling gas from the massive filaments to the left and right of Rex. Because these filaments are so large the gas in-falling from the other filament above Rex gets dwarfed, and in comparison the area around Rex behaves similarly to a filament. The key difference is that Rex isn't actually part of a filament, but is at the meeting place of two massive filaments. This was confirmed when we looked at present time and Rex as well as the other halos switched back to being classified as clusters. Rex grows to

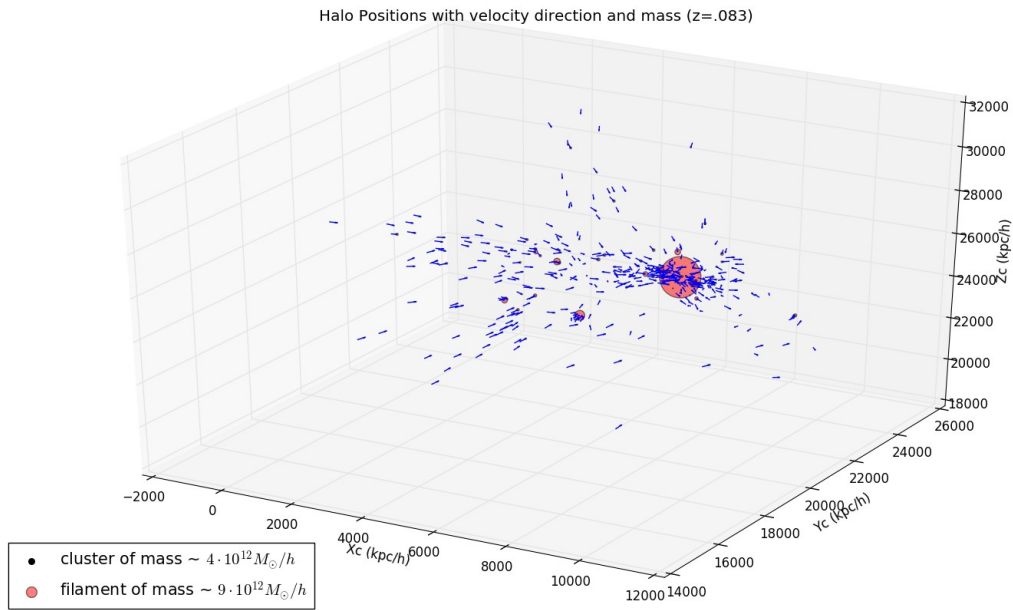


Figure 7: Halo positions with velocity direction denoted by arrows. Black halos are in clusters and red halos are in filaments.

a mass of $1.59 \cdot 10^{14} M_{\odot}/h$ and contains 95 subhalos by present time.

At this point we reexamined the large system as a whole over the entire redshift while looking for changes in the massive halos. To allow us to look at the system through all redshifts we graphed the system at 4 different redshifts in Figures 8, 9, 10, and 11 below.

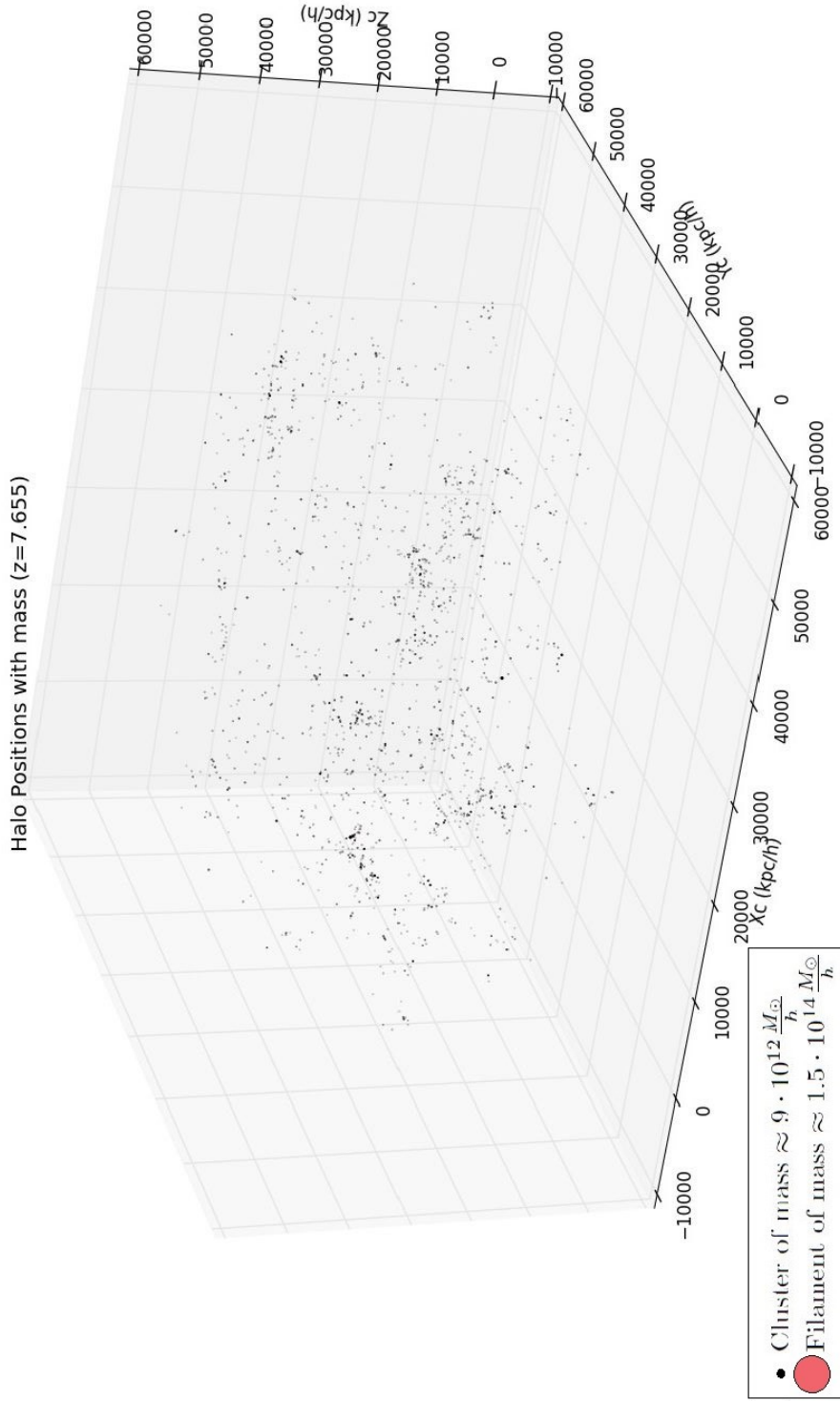


Figure 8: Halo position and mass at varying redshifts. Black halos are in clusters and red halos are in filaments.

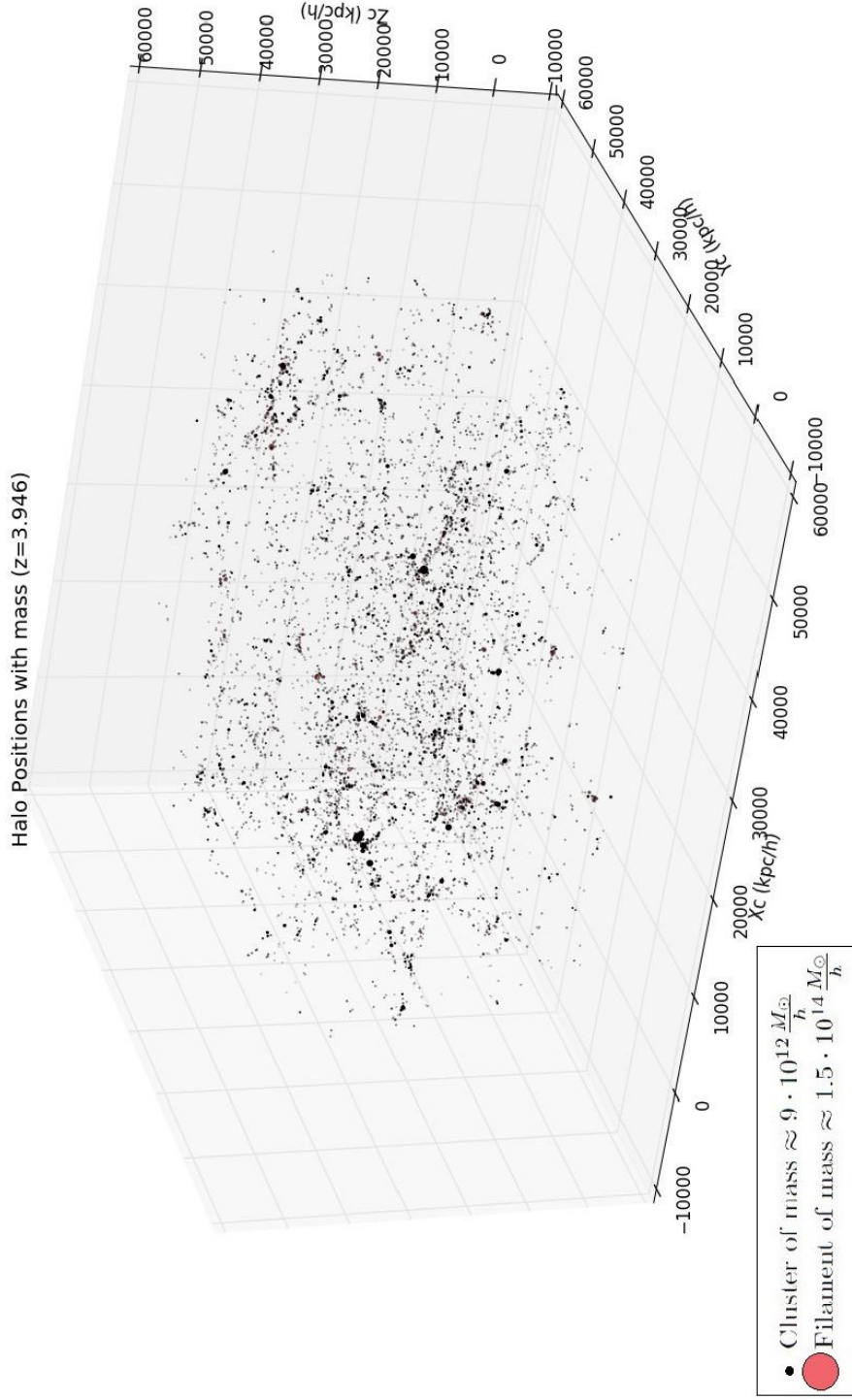


Figure 9: Halo position and mass at varying redshifts. Black halos are in clusters and red halos are in filaments.

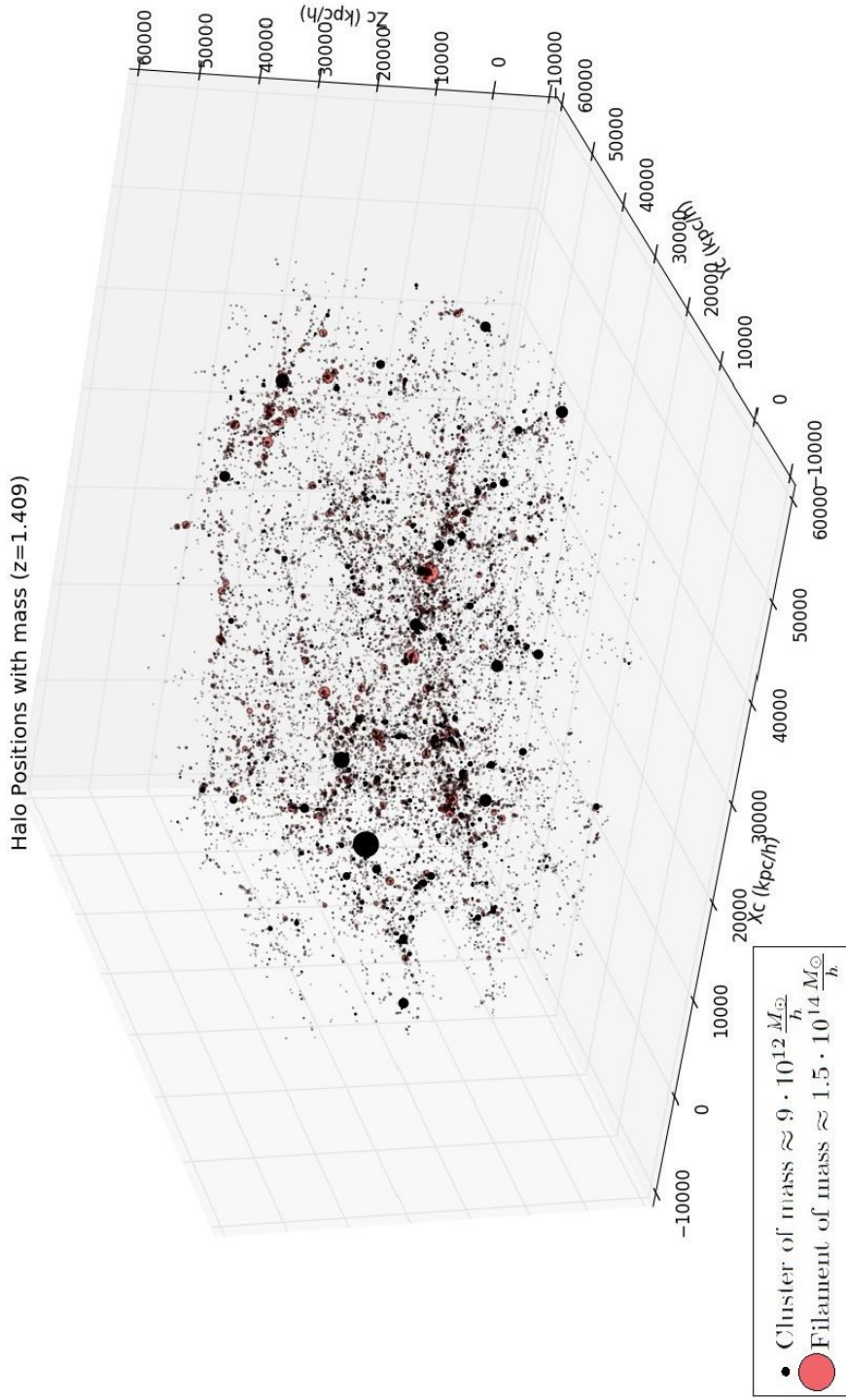


Figure 10: Halo position and mass at varying redshifts. Black halos are in clusters and red halos are in filaments.

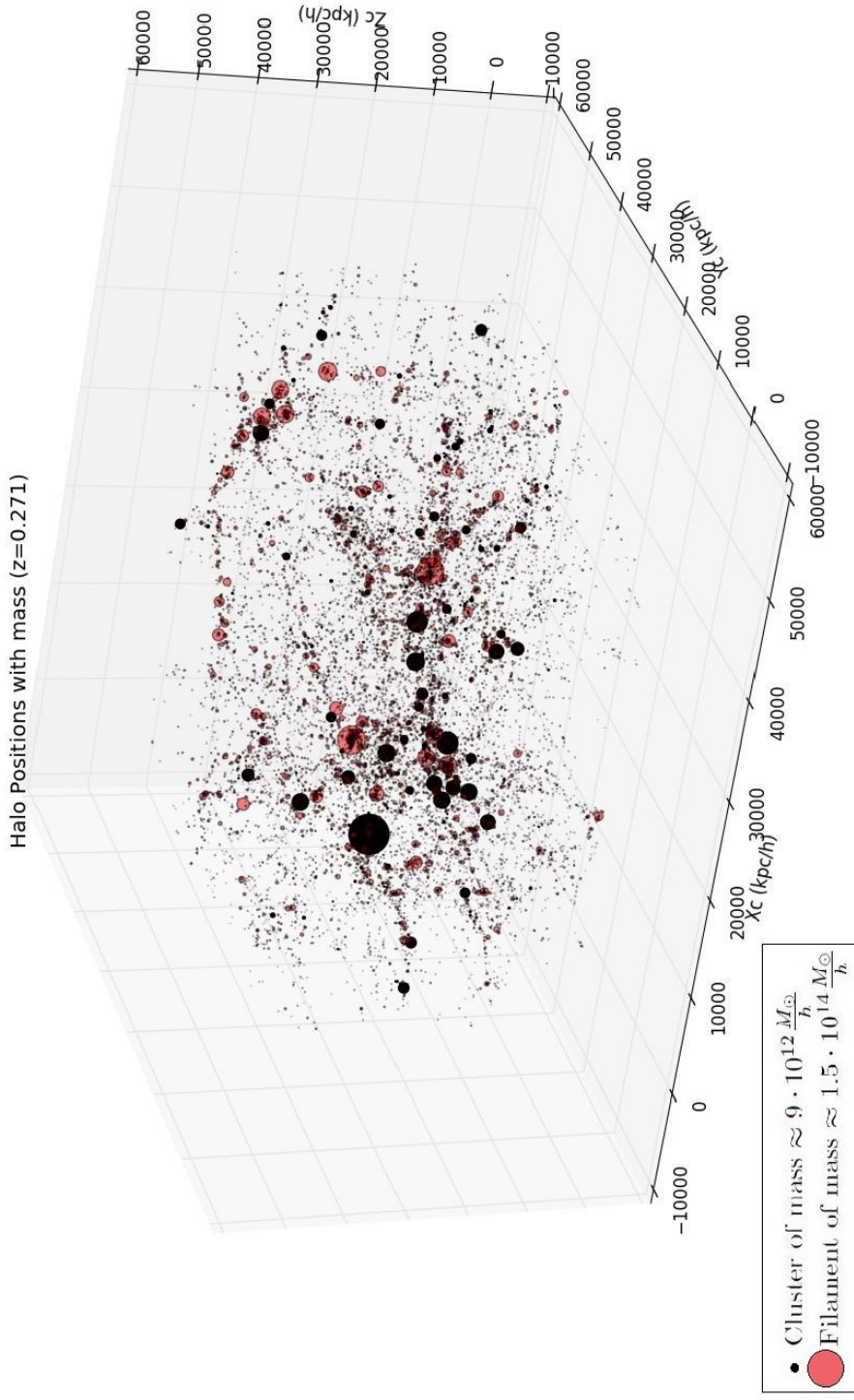


Figure 11: Halo position and mass at varying redshifts. Black halos are in clusters and red halos are in filaments.

As we look at Figures 8, 9, 10, and 11 we see that these massive halos can be seen forming at high redshifts and continue growing as the space around them fills with other smaller halos. Additionally, we also see the filaments of halos forming around these massive halos. Closer examination shows that these massive halos move towards each other and given enough time they would likely merge together to form a super massive halo.

6 Future work

In order for this research to continue on its current path we must develop a way to track halos between redshifts. Until we create this tool we will have to examine the halos without the knowledge of which halos are likely infalling and which are not. The development of a halo tracking tool will allow us to examine the differences between infalling halos and other halos. We can then start to discover what halos tend to infall into the clusters at the cosmic nodes and which will remain outside.

7 Conclusion

I developed tools to graphically analyze the halos found using AHF on the output of a GADGET 2 large scale universe simulation. I then used these tools to show how halos moved through different regions of space and changed classification as time passed. From this we see that the large scale structure of the universe is still changing with halos continuing to be created and growing in mass up to present time.

References

- [1] Knebe, Alexander. *AHF - AMIGA's Halo Finder. 1st ed. 2014. Web. 23 Mar. 2017.*
- [2] Bullock, J. S., et al., (2001). *A Universal Angular Momentum Profile for Galactic Halos. Retrieved from <http://iopscience.iop.org/article/10.1086/321477/pdf>*
- [3] Peebles, P. J. E. 1980, *Research supported by the National Science Foundation. Princeton, N.J., Princeton University Press, 1980. 435 p.,*
- [4] Snedden, A., et al., (2015). *A new Multi-Scale Structure Finding Algorithm to Identify Cosmological Structure. Retrieved from <http://arxiv.org/pdf/1409.7711v1.pdf>*
- [5] Snedden, A., et al., (2016). *Star formation and gas phase history of the cosmic web. Monthly Notices of the Royal Astronomical Society, Volume 455, Issue 3, p.2804-2825*
- [6] Springel V., 2005, *MNRAS, 364, 1105*
- [7] Springel V., Yoshida N., White S. D. M., 2001, *New Astronomy, 6, 79*
- [8] Turk, M. J., et al., (2011). *yt: A Multi-code Analysis Toolkit for Astrophysical Simulation Data The Astrophysical Journal Supplement, Volume 192, Issue 1, article id. 9, p.16.*
- [9] Teklu, A., Remus, R., Dolag, K., & Burkert, A. (2014). *The Angular Momentum Dichotomy. Retrieved from http://wwwmpa.mpa-garching.mpg.de/HydroSims/Magneticum/Proceedings/teklu_iau309.pdf*